LIL3, a light-harvesting-like protein, plays an essential role in chlorophyll and tocopherol biosynthesis

Ryouichi Tanaka[a,1], Maxi Rothbart[b], Seiko Oka[c], Atsushi Takabayashi[a], Kaori Takahashi[a], Masaru Shibata[d], Fumiyoshi Myouga[e], Reiko Motohashi[f], Kazuo Shinozaki[e], Bernhard Grimm[b], and Ayumi Tanaka[a]

[a]Institute of Low Temperature Science, Hokkaido University, Sapporo 060-0819, Japan; [b]Institute of Biology/Plant Physiology, Humboldt University, D 10115 Berlin, Germany; [c]Instrumental Analysis Division, Equipment Management Center, Creative Research Institute, Hokkaido University, Sapporo 060-0812, Japan; [d]Department of Materials Engineering, Nagaoka National College of Technology, Niigata 940-8532,Japan; [e]RIKEN Plant Science Center, Yokohama, Kanagawa 230-0045, Japan; and [f]Faculty of Agriculture, Shizuoka University, Shizuoka 422-8529, Japan

Edited by Diter von Wettstein, Washington State University, Pullman, WA, and approved August 5, 2010 (received for review April 7, 2010)

The light-harvesting chlorophyll-binding (LHC) proteins are major constituents of eukaryotic photosynthetic machinery. In plants, six different groups of proteins, LHC-like proteins, share a conserved motif with LHC. Although the evolution of LHC and LHC-like proteins is proposed to be a key for the diversification of modern photosynthetic eukaryotes, our knowledge of the evolution and functions of LHC-like proteins is still limited. In this study, we aimed to understand specifically the function of one type of LHC-like proteins, LIL3 proteins, by analyzing *Arabidopsis* mutants lacking them. The *Arabidopsis* genome contains two gene copies for LIL3, *LIL3:1* and *LIL3:2*. In the *lil3:1/lil3:2* double mutant, the majority of chlorophyll molecules are conjugated with an unsaturated geranylgeraniol side chain. This mutant is also deficient in α-tocopherol. These results indicate that reduction of both the geranylgeraniol side chain of chlorophyll and geranylgeranyl pyrophosphate, which is also an essential intermediate of tocopherol biosynthesis, is compromised in the *lil3* mutants. We found that the content of geranylgeranyl reductase responsible for these reactions was severely reduced in the *lil3* double mutant, whereas the mRNA level for this enzyme was not significantly changed. We demonstrated an interaction of geranylgeranyl reductase with both LIL3 isoforms by using a split ubiquitin assay, bimolecular fluorescence complementation, and combined blue-native and SDS polyacrylamide gel electrophoresis. We propose that LIL3 is functionally involved in chlorophyll and tocopherol biosynthesis by stabilizing geranylgeranyl reductase.

Arabidopsis | phytol | geranylgeranyl reductase | tetrapyrrole

Light-harvesting chlorophyll-binding (LHC) proteins are major components of the eukaryotic photosynthetic machinery and form the outer antenna protein complexes of photosystem (PS) I and II in chloroplasts. Each LHC protein typically binds approximately a dozen chlorophyll (Chl) molecules and three to four different carotenoids (1) and, thus, plays essential roles in photosynthesis and photoprotection. LHC protein harvests light energy and transfers the excitation energy to the photosynthetic reaction center.

Cyanobacteria contain small groups of single-helix proteins with LHC motifs. These proteins are suggested to function in the stabilization of PS I (2) and in the protection of Chl against Chl-degrading enzymes during the assembly and repair of PS II (3, 4). Eukaryotic LHC proteins are proposed to evolve from a cyanobacterial single-helix progenitor (5–7). At present, the exact functions of recent cyanobacterial LHC-like proteins and the hypothetical ancestral LHC-like protein remain elusive. During the evolution of eukaryotic photosynthesis, it is likely that the ancestral protein united with another membrane-spanning protein. As a result of subsequent gene duplication and deletion, it may have differentiated into various types of LHC and LHC-like proteins to become widely distributed among photosynthetic eukaryotes (5, 6, 8, 9). Typical eukaryotic LHC have three membrane-spanning helices, whereas LHC-like proteins contain one to four membrane-spanning domains (10). *Arabidopsis thaliana* contains 10 abundant and a few rarely expressed LHC (10–12). In addition, it contains a total of 10 LHC-like proteins, including three single-helix proteins [OHP1, OHP2, and ferrochelatase2 (FeC2)], four double-helix proteins (SEP1, SEP2, LIL3:1, and LIL3:2), two three-helix proteins (ELIP1 and ELIP2), and one four-helix protein (PsbS). All of these LHC-like proteins share a membrane-spanning consensus sequence, the LHC motif (10), which is ~25-aa residues long and contains a few conserved basic residues, although the residual residues are mostly hydrophobic.

The conserved structure of the LHC-like proteins is apparently most widely distributed among eukaryotic photosynthetic organisms and implicates their involvement in essential processes. The primary role of the LHC motif in the major LHC proteins is to provide ligands for Chl binding and to enable energy transfer among Chl molecules for photosynthesis (1). It is intriguing that this motif is widely used in a number of divergent proteins, and it can be speculated that this motif has a unique and unidentified function that is shared by the LHC-like proteins including OHP, SEP, ELIP, and FeC2. Diversification of these LHC family proteins has most likely contributed to the successful environmental adaptation of photosynthetic eukaryotes (7). Understanding the functions of LHC-like proteins may allow us to predict a common function of the LHC motif. Furthermore, it may also provide insight into the evolutionary history of these organisms adapting to their habitats (5, 7, 13).

To date, the functions of two LHC-like proteins (PsbS and FeC2) have been determined. PsbS plays an essential role in nonphotochemical quenching in land plants (14). FeC2 is one of the two ferrochelatase isoforms that catalyze the last step of heme biosynthesis by incorporating Fe^{2+} into protoporphyrin IX to produce protoheme. The functions of other LHC-like proteins remain poorly understood. OHP, SEP, and ELIP proteins are proposed to be involved in protection against excessive light. The expression of the genes for these proteins is induced under strong illumination (15–19). In addition, it has also been suggested that ELIP functions as a repressor of chlorophyll biosynthesis (20).

In contrast, LIL3 may not be related to light protection because the expression of the *LIL3* genes does not seem to be inducible by strong illumination according to the Nottingham Arabidopsis Stock Center microarray database (21). Instead, LIL3 is proposed to transfer de novo synthesized Chl to the photosystems because it is associated with pigment-binding proteins that appear temporally at the greening stage of barley

Author contributions: R.T., B.G., and A. Tanaka designed research; R.T., M.R., S.O., A. Takabayashi, and K.T. performed research; F.M., R.M., and K.S. constructed a new and specific mutant pool of *Arabidopsis*; R.T., S.O., and M.S. analyzed data; and R.T. and B.G. wrote the paper.

The authors declare no conflict of interest.

This article is a PNAS Direct Submission.

[1]To whom correspondence should be addressed. E-mail: rtanaka@lowtem.hokudai.ac.jp.

This article contains supporting information online at www.pnas.org/lookup/suppl/doi:10.1073/pnas.1004699107/-/DCSupplemental.

seedlings (22). It is possible that LIL3 has a unique biological function that is distinct from those of other LHC-like proteins.

To elucidate the function of LIL3 proteins, we analyzed *A. thaliana* transposon mutants lacking one or both isoforms of LIL3 proteins. These mutants are impaired in the synthesis of α-tocopherol and phytylated Chl. This misregulation is a consequence of a reduced content of geranylgeranyl reductase (GGR). This enzyme is responsible for the reduction step of geranylgeranyl pyrophosphate (GGPP) to phytyl pyrophosphate (phytyl-PP) (23, 24), which is required for Chl, tocopherol, and phyloquinone biosynthesis. We demonstrated a physical interaction of LIL3 and GGR, suggesting that LIL3 stabilizes GGR in plastid membranes.

Results

Characterization of the Two *LIL3* Genes from *A. thaliana*. The *Arabidopsis* genome contains two *LIL3* genes, At4g17600 and At5g47110, which we tentatively named *LIL3:1* and *LIL3:2* genes. These genes encode proteins of 262 and 258 aa, respectively. A computer program, ChloroP, which specializes in the prediction of transit peptides (25), predicted that 39 and 42 aa residues of the N-terminal sequences of LIL3:1 and LIL3:2 are transit peptides, which facilitate the import of these proteins into the plastid. According to these predictions, mature sizes of LIL3:1 and LIL3:2 are predicted to be 25.1 and 24.1 kDa, respectively. These two proteins share 85% similarity and 76% identical amino acids. The structure-prediction programs HMMTOP (26) and TMHMM (27) indicate two membrane-spanning helices, among which the first helix of LIL3 proteins includes the well-conserved LHC motif (Fig. S1).

LIL3 homologs can be found exclusively in organisms belonging to the green lineage of the photosynthetic eukaryotes. A phylogenetic analysis indicates that the *Arabidopsis* pair of the angiosperm *LIL3* homologs arose very recently, at least after the divergence of mono- and dicotyledonous plants (Fig. S2).

***lil3* Mutants Are Compromised in the Biosynthesis of Chl_{phytol}.** For better understanding of tetrapyrrole metabolism in plants, Tanaka's group at the Hokkaido University has conducted large-scale HPLC-based screening programs to identify pigment biosynthesis mutants (28). In this screening project, we identified two *Arabidopsis* mutant lines, Ds13-3953 and Ds13-0193, from the Riken Institute (Japan) *Dissociation* (*Ds*)-tagged lines (29), which accumulated unusual Chl species as described below. In Ds13-3953 and Ds13-0193, the *Ds* transposon was inserted into the first exons of the *LIL3:1* and *LIL3:2* genes, respectively, which very likely abolished the functions of these proteins. Hereafter, the two mutant lines are referred to as *lil3:1* and *lil3:2*, respectively. In addition to the insertion in the *LIL3:2* gene, another copy of the transposon was inserted into the upstream intergenic region of At5g43196, which was predicted to be a pseudogene according to the annotation of the Arabidopsis Information Resource (TAIR; http://www.arabidopsis.org/). We crossed *lil3:1* and *lil3:2* to obtain the *lil3:1/lil3:2* double mutant.

The sizes and leaf colors of *lil3:1* and *lil3:2* mutants were indistinguishable from those of WT under our experimental growth conditions of 23 °C and light intensity of ~80 μmol photons m^{-2} s^{-1} (Fig. S3). In contrast, the *lil3:1/lil3:2* double mutant exhibited yellowish green leaves and grew slower than the *lil3:1, lil3:2*, and WT plants (Fig. S3). It is assumed that LIL3:1 and LIL3:2 proteins share overlapping functions and that the deficiency of both LIL3 isoforms results in the phenotypical difference from WT.

We analyzed the pigment compositions of the *lil3* mutants by HPLC. Detailed information on pigment identification is shown in Fig. S4. In all of the *lil3* mutants, Chl *a* and Chl *b* species are conjugated with incompletely reduced side chains including tetrahydrogeranylgeraniol (THGG), dihydrogeranylgeraniol (DHGG), and geranylgeraniol (GG) in addition to normal phytylated Chl *a* (Chl a_{phy}) and Chl *b* (Chl b_{phy}). (Fig. 1*A*). In *lil3:1* and *lil3:2*, a minor fraction of Chl *a* and Chl *b* contained the incompletely reduced side chains (Fig. 1*A*). Three percent of Chl in *lil3:1* and 16% in *lil3:2* were conjugated with incompletely reduced side chains (GG, DHGG, and THGG) among which Chl_{THGG} was the most abundant (Fig. 1*B*). In contrast, in the *lil3:1/lil3:2* mutant, the majority (96%) of Chl molecules are conjugated with either THGG, DHGG, or GG. (Fig. 1*B*). These results indicate that LIL3 proteins are required for complete biosynthesis of phytylated Chl molecules in green seedlings.

Lack of LIL3 Proteins Compromises the Stability of GGR. In plants, Chl_{phy} is synthesized via two routes (reviewed in ref. 30). GGPP is esterified with chlorophyllide (Chlide) to form Chl_{GG} and is subsequently reduced stepwise to Chl_{phy}. Alternatively, GGPP can be first reduced to phytyl-PP before it is conjugated with Chlide. GGR is an NADPH-dependent enzyme and is responsible for the reduction of GGPP to phytyl-PP and the reduction of Chl_{GG} to Chl_{phytol} (23, 24). This enzyme is encoded by the *CHLP* gene (At1g74470). It has been reported that reduced expression of *CHLP* in tobacco leads to the accumulation of Chl_{GG}, Chl_{DHGG}, and Chl_{THGG} species in plants (24). Thus, we speculated that the level of GGR might be affected in the *lil3* mutants and examined

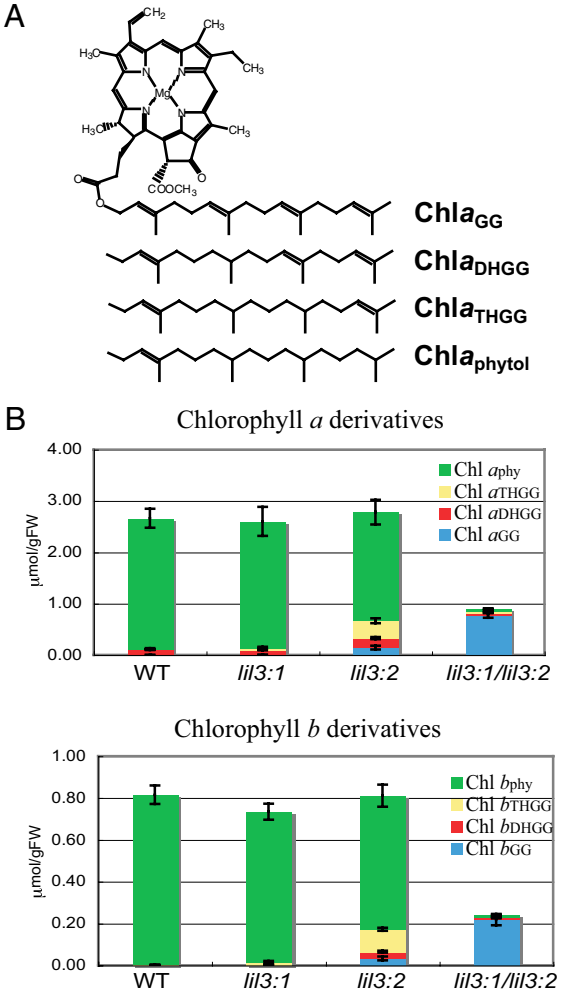

Fig. 1. Accumulation of Chl and its derivatives that are characterized by the conjugation of incompletely reduced side chains. (*A*) Chemical structure of Chl *a* derivatives that are conjugated with either GG, DHGG, THGG, or phytol. (*B*) The contents of Chl *a* and Chl *b* derivatives in WT, *lil3:1, lil3:2*, and *lil3:1/lil3:2* plants that were grown for 4 wk as described in *Materials and Methods*. Error bars indicate SD (n = 5).

CHLP expression at the transcript and protein level by real-time (RT)-PCR and immunoblotting, respectively.

The *CHLP* mRNA levels were not significantly altered in the *lil3* mutants relative to WT (Fig. 2*A*). In contrast, the GGR levels were reduced in all *lil3* mutants and were barely detectable in leaf extracts of *lil3:1/lil3:2* (Fig. 2). [Note: when the antibody concentration of the anti-GGR antibody was increased 2-fold, a weak immunoreactive signal was detected despite a high-background signal intensity (Fig. S5).] Thus, LIL3 deficiency does not affect *CHLP* gene expression, but LIL3 is involved in the stabilization of GGR.

Absence of LIL3 Proteins Led to Tocopherol Deficiency. Phytyl-PP forms also the hydrophobic carbohydrate side chain of tocopherol molecules. Reduction in the GGR content has been reported to be associated with tocopherol deficiency in tobacco (24). To explore further consequences of reduced GGR levels in response to lack of LIL3 proteins, we examined the α-tocopherol contents in the *lil3* mutants (Fig. 3 and Fig. S6). Compared with WT, the tocopherol levels of *lil3:1* and *lil3:2* were not significantly altered. In contrast, almost no α-tocopherol accumulated in the double mutant (Fig. 3 and Fig. S6). The possibility that the tocochromanol ring is esterified with GG instead of phytol to form α-tocotrienol, which was detected in a *CHLP* insertional mutant of *Synechosystis* PCC6803 lacking phytylated Chl and α-tocopherol (31), cannot be ruled out. However, as in tobacco *CHLP*-antisense RNA-expressing plants (24), accumulation of α-tocotrienol, whose elution time was ∼4 min in our HPLC system, was barely detectable in the *lil3* mutants (Fig. S6). It was previously suggested that the *Arabidopsis* homogentisic acid geranylgeranyl transferase, catalyzing the conjugation of tocochromanol and the isoprenoid side chain, preferentially uses phytyl-PP as a substrate, whereas the same enzyme from barley is able to produce both phytylated and geranylgeranylated tocochromanols (32). These results further support our conclusion that a lack of LIL3 leads to reduced GGR activity.

Interaction of GGR and LIL3. The aforementioned results confirm that GGR constantly accumulates only when either or both LIL3:1 and LIL3:2 are present. Because both LIL3 and GGR are localized in thylakoid membranes (33), we speculate that a stable accumulation of GGR is achieved by a direct interaction between LIL3 and GGR. We examined such an interaction with a yeast split ubiquitin assay and a bimolecular fluorescence complementation assay (BiFC), and analyzed the in vivo complex formation with the blue-native polyacrylamide gel electrophoresis (BN-PAGE).

The split ubiquitin assay can be efficiently applied to detect the interaction of a membrane-bound bait protein with a prey protein (34). In this assay with GGR fused to the N-terminal half of ubiquitin and either LIL3:1 or LIL3:2 fused to the C-terminal half of ubiquitin, a protein–protein interaction was specifically detected (Fig. 4*A*). Sucrose transporter 1 of potato (SUT1) was used as a negative control, which failed to give rise to any colony growth with either GGR, LIL3:1, or LIL3:2 (Fig. 4*A*).

For the BiFC assay in tobacco leaves, we transiently expressed GGR conjugated with the N-terminal half of Venus (a variant of green fluorescent protein) and either LIL3:1 or LIL3:2, which were conjugated with the C-terminal half of Venus. A combination of GGR and either LIL3:1 or LIL3:2 resulted in Venus fluorescence in chloroplasts, indicating a physical interaction of these proteins within the chloroplasts (Fig. 4*B*). Conversely, the vector-only negative control failed to emit fluorescent signals.

In vivo complex formation of GGR and LIL3 proteins was examined by analyzing protein complexes from thylakoid membranes that were solubilized with 1% β-dodecylmaltoside and separated by BN-PAGE. The proteins were subsequently analyzed by SDS/PAGE in 2D and resolved proteins were detected with immunoblotting (Fig. 4*C*). The anti-GGR antibody generated signals at ∼170 kDa and in the range of low molecular weight proteins corresponding to 50 kDa or less. The same antibody also gave trailing signals between an approximate size range of 50 kDa, at around 80 kDa, and several faint spots above 200 kDa. These signals could be the result of nonspecific binding of the antibody or they may represent the formation of large (>200 kDa) multiple protein complexes of GGR. The LIL3 antibody gave three major spots at <50-, 80-, and 170-kDa positions (Fig. 4*C*). The BN-PAGE analysis indicates that GGR and LIL3 proteins are present as monomers and assemble in high-molecular-weight protein complexes. It is possible that the 170-kDa complex contains both GGR and LIL3 proteins simultaneously.

Discussion

In this report, we demonstrate that LIL3 is required for stable accumulation of GGR and can conclude that it is functionally involved in Chl and tocopherol biosynthesis. It is speculated that the conserved LHC motif of LIL3 contributes to the stability and function of GGR by tentative binding of Chl_{GG} that supports the enzymatic reaction of GGR. This scenario is apparently contradictory to a previous report in which recombinant plant GGR is shown to complete the three-step reduction of GGPP (or Chl_{GG}) to phytyl-PP (or Chl_{phytol}) in vitro without LIL3 (23). However, it is also possible that LIL3 could enhance the activity of GGR in vivo. Another possible function of LIL3 may be tethering GGR to plastid membranes. Although GGR was detected in thylakoid and envelope membranes during recent proteomic analyses (35), this protein does not possess predictable transmembrane regions (23). Because LIL3 is an obvious membrane-spanning protein, it is reasonable to assume

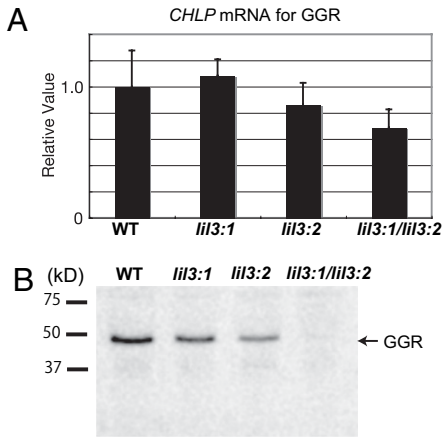

Fig. 2. (*A*) Quantification of *CHLP* mRNA levels analyzed with RT-PCR analysis. The mRNA levels were normalized by those of *UBC21* mRNA encoding ubiquitin-conjugating enzyme 21 for each sample. The *CHLP* mRNA levels in the mutants were shown relative to WT. Error bars indicate SD ($n = 3$). $P > 0.05$ in all pairwise comparison with a nonparametric Student *t* test. (*B*) Protein extracts equivalent to 0.5 mg leaf tissue were loaded per lane and detected with anti-GGR antiserum (8,000× dilution) as described in *Materials and Methods*. An arrow indicates the immunologically-detected signals of GGR.

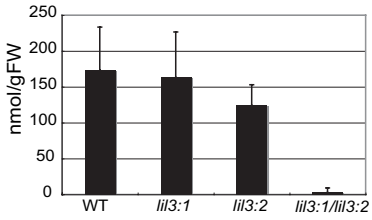

Fig. 3. Quantification of α-tocopherol in WT, *lil3:1*, *lil3:2*, and *lil3:1/lil3:2*. Error bars indicate SD ($n = 3$). $P > 0.05$ between WT and either *lil3:1* or *lil3:2* in pairwise comparison with a nonparametric Student's *t* test. The α-tocopherol in the *lil3:1/lil3:2* double mutant was below a quantifiable level.

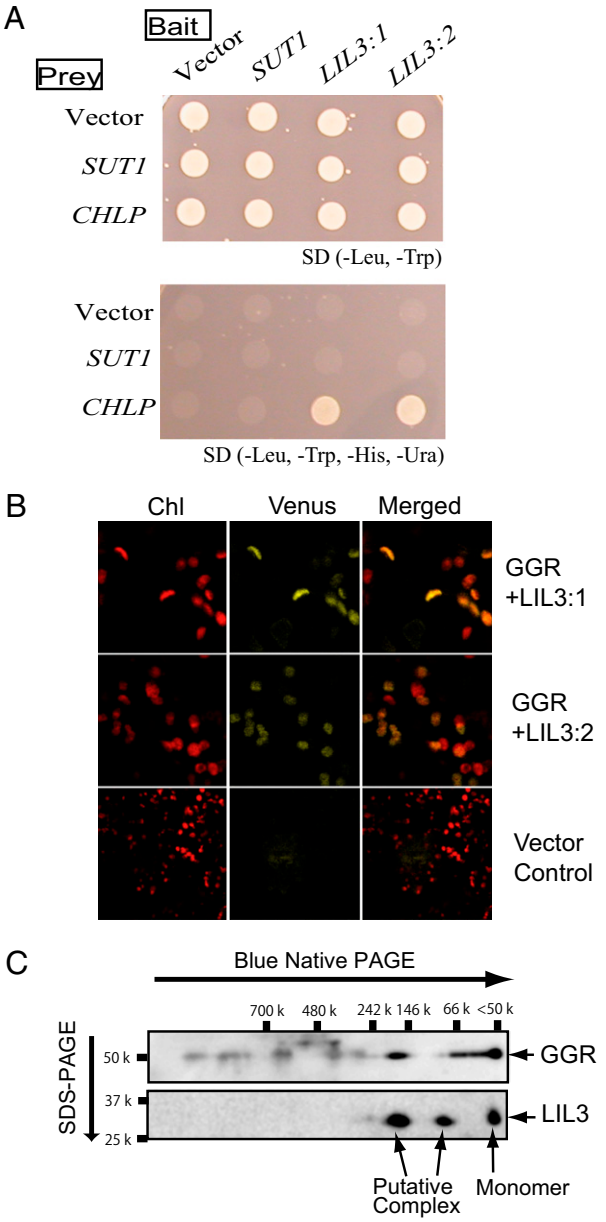

Fig. 4. To detect the interaction of LIL3 and geranylgeranyl reductase, a split ubiquitin assay (*A*), an in vivo BiFC assay (*B*), and BN-PAGE analyses were performed. (*A*) Split ubiquitin assay: pCub bait vectors harboring no insert (Vector), *SUT1*, *LIL3:1*, or *LIL3:2* cDNA clones were introduced into the Lcc40uA yeast strain. pNub prey vectors harboring no inserts (Vector), *SUT1*, or *CHLP* cDNA clones were introduced into the same strain. A double transformation with pNub and pCub vectors enabled all transfomants to grow on synthetic defined medium lacking Leu and Trp. In contrast, on synthetic defined medium lacking Leu, Trp, His, and Ura, only transformants harboring *CHLP* and *LIL3:1* or *LIL3:2* were able to grow. (*B*) A BiFC assay demonstrated the interaction of GGR and LIL3 proteins in chloroplasts. Chlorophyll fluorescence (*Left*, top two images) represents the chloroplasts within cells. Combined expression of fusion proteins containing GGR and either LIL3:1 or LIL3:2 results in Venus fluorescence (*Center*, top two images). The restored Venus fluorescence colocalizes with chlorophyll fluorescence (*Right*, top two images). A combination of empty NUB and CUB vectors did not lead to Venus fluorescence (*Bottom*). (*C*) BN-PAGE analysis combined with SDS/PAGE and immunoblotting indicates that GGR and LIL3 can be detected in a 170-kDa protein complex. Both proteins can be detected also as monomers or in other protein complexes.

that interaction with GGR may anchor this protein to the membranes. Such membrane localization of GGR is advantageous for the access of GGR to its hydrophobic isoprenoid substrates.

We also hypothesized that the LIL3–GGR interaction is linked to the reported changes in the substrate selectivity of GGR at different developmental stages (36). At the deetiolation stage, GGR reacts with Chl_{GG} to form Chl_{phytol}, whereas in green leaves, GGR appears to react with GGPP and convert it into phytyl-PP, the substrate for Chl and tocopherol formation (36). Our hypothesis is supported by the observation that LIL3 is a major component of protein complexes that contains a precursor of Chl biosynthesis and specifically appears during the deetiolation stage of barley seedlings (22). These complexes in barley were estimated to have molecular masses around 160–180 kDa and 210–250 kDa (22). It is possible that at least one of these complexes corresponds to one of the LIL3 protein complexes in *Arabidopsis* (Fig. 4*C*). It is tempting to speculate, as hypothesized by Reisinger et al. (22), that this complex is involved in the conversion of protochlorophyllide to Chl_{phytol} via Chl_{GG}, and/or that this complex contains GGR and other enzymes that are necessary for Chl biosynthesis in addition to LIL3. Because our knowledge of controlled metabolic channeling for phytol biosynthesis is still limited, our findings about LIL3 functions will become an essential step toward a comprehensive understanding of these plastidic processes.

Considering the significant conservation of the LHC motif among many plastid proteins (10) (Fig. S1), it would be reasonable to assume that this motif has common functions among these proteins. Because known functions of LHC proteins include their ability to carry Chl and carotenoids and to move between different protein complexes (37), it is reasonable to consider that a common function of the LHC motif is to facilitate a reversible protein–protein interaction. Ferrochelatase (38), OHP (32), and ELIP (32) have been experimentally shown or proposed to interact with different proteins. It would be tempting to speculate that an LHC motif functions to switch proteins between different protein complexes.

Including our results showing the involvement of LIL3 in Chl biosynthesis, three (LIL3, FeC2, and ELIP) out of six different plant LHC-like proteins have been reported to contribute to tetrapyrrole biosynthesis (10, 20). Because most tetrapyrrole molecules are photosensitizing and potentially phototoxic to plant cells (39), efficient channeling of the biosynthetic intermediates and the final tetrapyrrole products to their final destination should be an essential process in plant cells. Findings from this study suggest that plants harness LHC-like proteins for efficient control of the metabolic pathways.

Materials and Methods

Plant Materials and Growth Conditions. The *lil3:1* and *lil3:2* mutants were isolated from a *Ds* transposon-tagged mutant pool of the Nossen ecotype (29). Plants were grown at 23 °C under continuous light conditions [~80 μmol m^{-2} s^{-1} on a 3:1 mixture of vermiculite and nourished soil (Sankyo-Baido soil; Hokkai-Sankyo Co. Ltd.)]. The fourth whorl of the leaves counting from the top was harvested 4 wk after germination for extraction of pigments, RNA, and protein.

Measurement of Chls and Tocopherols by HPLC. Chls and tocopherols were extracted from frozen leaves with acetone and subjected to HPLC analysis. Chls were separated on a Waters C8 column (Symmetry C8, 150 mm × 4.6 mm, 3.5-μm particle size) as previously described (28). Tocopherols were also separated according to the previously described method (24) with minor modifications. Instead of using the C18 column as described in the original method, we used a C8 column (Symmetry C8), which resulted in a faster separation of tocopherol derivatives. α-tocopherol was excited at 290 nm and fluorescence was monitored at 320 nm with a fluorescent detector (L-2485; Hitachi Hi-Tech Corp.). Pigments were quantified by use of standard pigments. Chl *a* and Chl *b* were purchased from Juntec Co. Ltd, and α-tocopherol and α-tocotrienol from Wako Pure Chemical Industries and Cayman Chemical, respectively.

RT-PCR and Immunoblotting. Detailed description on the methodology of RT-PCR was provided in *SI Materials and Methods*. Briefly, cDNA was synthesized from 1 μg of total RNA with the PrimeScript RT reagent kit (Takara Bio Inc.) and amplified with Sybr Premix Ex Taq (Takara Bio Inc.) according to the manufacturer's instruction using the following pair of primers for the coding

regions for *CHLP*. The amplicon was quantified with LightCycler (Roche Diagnostics K. K.). The relative levels of *CHLP* mRNA were normalized by the levels of *UBC21* (At5g25760). For immunoblotting, total leaf protein was extracted from the fourth whorl of 4-wk-old plants with extraction buffer containing 50 mM Tris-HCl pH 6.8, 2 mM EDTA, 10% glycerol, 2% SDS, and 6% 2-mercaptoethanol. Five microliters of extracts, corresponding to 0.5 mg of leaf material, were separated on a 14% polyacrylamide gel and electroblotted to PVDF membrane. The GGR protein was detected with an anti-GGR antiserum (24) using the ECL Plus immunodetection kit (GE Healthcare).

Split Ubiquitin Assay. The coding sequences of *LIL3:1* and *LIL3:2* were cloned into the pCub bait vector (Dualsystems Biotech AG). The coding sequence of *CHLP* was cloned into the pNub prey vector (Dualsystems Biotech AG). As negative controls of the prey and bait vectors, we used *SUT1* that was cloned into pCub and pNub vectors (34). In vivo interaction of the proteins encoded in the prey and bait vectors facilitated growth of the colonies on synthetic defined media lacking leucine, tryptophan, histidine, and uracil. Detailed methodology for this assay is provided in *SI Materials and Methods*.

BiFC Assay. Coding regions of *ChlP, LIL3:1*, and *LIL3:2* from *A. thaliana* cDNA were cloned into destination vectors pDEST-^{GW}VYNE for *LIL3:1* and *LIL3.2* and pDEST-^{GW}VYCE (40) for *CHLP*, respectively. These constructs were transiently transformed to *Nicotiana benthamiana* leaves with *Agrobacterium tumefaciens* GV2260. Plants were kept 3 d in dark before analyses of infected leaf disks by confocal microscopy (excitation 514 nm, emission Venus 525–600 nm, emission chlorophyll 620–700 nm).

BN-PAGE Analysis. The isolation of thylakoid membranes and BN-PAGE was performed according to the methods described by Wittig et al. (41). Briefly, thylakoid membrane proteins isolated from 4-wk-old leaves (corresponding to 10 μg of chlorophyll) were solubilized with 1% (wt/vol) dodecyl maltoside on ice for 5 min in resuspension buffer [50 mM imidazole-HCl (pH 7.0), 20% glycerol, 5 mM 6-aminocaproic acid, 1 mM EDTA]. Solubilized membrane proteins were then separated by 4–13% acrylamide gradient gels. Native-Mark unstained molecular weight markers (Invitrogen) were used for estimation of protein size.

ACKNOWLEDGMENTS. We thank Sachiko Tanaka for her excellent technical assistance with the HPLC analysis and molecular biology techniques. This work was supported by Grants-in-Aid for Creative Scientific Research 17GS0314 (to A.T.) and 19687003 (to R.T.) from the Ministry of Education, Culture, Sports, Science, and Technology of Japan and a grant from the Deutsche Forschungsgemeinschaft-Research Unit 804 on Retrograde Signaling (to B.G.).

1. Liu Z, et al. (2004) Crystal structure of spinach major light-harvesting complex at 2.72 A resolution. *Nature* 428:287–292.
2. Wang Q, et al. (2008) The high light-inducible polypeptides stabilize trimeric photosystem I complex under high light conditions in Synechocystis PCC 6803. *Plant Physiol* 147:1239–1250.
3. Vavilin D, Yao D, Vermaas W (2007) Small Cab-like proteins retard degradation of photosystem II-associated chlorophyll in Synechocystis sp. PCC 6803: Kinetic analysis of pigment labeling with 15N and ^{13}C. *J Biol Chem* 282:37660–37668.
4. Vavilin D, Vermaas W (2007) Continuous chlorophyll degradation accompanied by chlorophyllide and phytol reutilization for chlorophyll synthesis in Synechocystis sp. PCC 6803. *Biochim Biophys Acta* 1767:920–929.
5. Green B, Pichersky E (1994) Hypothesis for the evolution of 3-helix Chl a/b and Chl a/c light-harvesting antenna proteins from 2-helix and 4-helix ancestors. *Photosynth Res* 39:149–162.
6. Green B, Kuhlbrandt W (1995) Sequence conservation of light-harvesting and stress-response proteins in relation to the 3-dimensional molecular-structure of LhcII. *Photosynth Res* 44:139–148.
7. Montané MH, Kloppstech K (2000) The family of light-harvesting-related proteins (LHCs, ELIPs, HLIPs): Was the harvesting of light their primary function? *Gene* 258:1–8.
8. Green BR, Durnford DG (1996) The Chlorophyll-Carotenoid Proteins of Oxygenic Photosynthesis. *Annu Rev Plant Physiol Plant Mol Biol* 47:685–714.
9. Koziol AG, et al. (2007) Tracing the evolution of the light-harvesting antennae in chlorophyll a/b-containing organisms. *Plant Physiol* 143:1802–1816.
10. Jansson S (1999) A guide to the Lhc genes and their relatives in Arabidopsis. *Trends Plant Sci* 4:236–240.
11. Klimmek F, Sjödin A, Noutsos C, Leister D, Jansson S (2006) Abundantly and rarely expressed Lhc protein genes exhibit distinct regulation patterns in plants. *Plant Physiol* 140:793–804.
12. Peng L, Fukao Y, Fujiwara M, Takami T, Shikanai T (2009) Efficient operation of NAD(P)H dehydrogenase requires supercomplex formation with photosystem I via minor LHCI in Arabidopsis. *Plant Cell* 21:3623–3640.
13. Adamska I, Ohad I, Kloppstech K (1992) Synthesis of the early light-inducible protein is controlled by blue light and related to light stress. *Proc Natl Acad Sci USA* 89: 2610–2613.
14. Li XP, et al. (2000) A pigment-binding protein essential for regulation of photosynthetic light harvesting. *Nature* 403:391–395.
15. Meyer G, Kloppstech K (1984) A rapidly light-induced chloroplast protein with a high turnover coded for by pea nuclear DNA. *Eur J Biochem* 138:201–207.
16. Grimm B, Kloppstech K (1987) The early light-inducible proteins of barley. Characterization of two families of 2-h-specific nuclear-coded chloroplast proteins. *Eur J Biochem* 167:493–499.
17. Heddad M, Adamska I (2000) Light stress-regulated two-helix proteins in Arabidopsis thaliana related to the chlorophyll a/b-binding gene family. *Proc Natl Acad Sci USA* 97:3741–3746.
18. Jansson S, Andersson J, Kim SJ, Jackowski G (2000) An Arabidopsis thaliana protein homologous to cyanobacterial high-light-inducible proteins. *Plant Mol Biol* 42: 345–351.
19. Andersson U, Heddad M, Adamska I (2003) Light stress-induced one-helix protein of the chlorophyll a/b-binding family associated with photosystem I. *Plant Physiol* 132: 811–820.
20. Tzvetkova-Chevolleau T, et al. (2007) The light stress-induced protein ELIP2 is a regulator of chlorophyll synthesis in Arabidopsis thaliana. *Plant J* 50:795–809.
21. Craigon DJ, et al. (2004) NASCArrays: A repository for microarray data generated by NASC's transcriptomics service. *Nucleic Acids Res* 32(Database issue):D575–D577.
22. Reisinger V, Plöscher M, Eichacker LA (2008) Lil3 assembles as chlorophyll-binding protein complex during deetiolation. *FEBS Lett* 582:1547–1551.
23. Keller Y, Bouvier F, d'Harlingue A, Camara B (1998) Metabolic compartmentation of plastid prenyllipid biosynthesis—evidence for the involvement of a multifunctional geranylgeranyl reductase. *Eur J Biochem* 251:413–417.
24. Tanaka R, Oster U, Kruse E, Rudiger W, Grimm B (1999) Reduced activity of geranylgeranyl reductase leads to loss of chlorophyll and tocopherol and to partially geranylgeranylated chlorophyll in transgenic tobacco plants expressing antisense RNA for geranylgeranyl reductase. *Plant Physiol* 120:695–704.
25. Emanuelsson O, Nielsen H, von Heijne G (1999) ChloroP, a neural network-based method for predicting chloroplast transit peptides and their cleavage sites. *Protein Sci* 8:978–984.
26. Tusnády GE, Simon I (2001) The HMMTOP transmembrane topology prediction server. *Bioinformatics* 17:849–850.
27. Krogh A, Larsson B, von Heijne G, Sonnhammer EL (2001) Predicting transmembrane protein topology with a hidden Markov model: Application to complete genomes. *J Mol Biol* 305:567–580.
28. Nagata N, Tanaka R, Satoh S, Tanaka A (2005) Identification of a vinyl reductase gene for chlorophyll synthesis in Arabidopsis thaliana and implications for the evolution of Prochlorococcus species. *Plant Cell* 17:233–240.
29. Myouga F, et al. (2010) The Chloroplast Function Database: A large-scale collection of Arabidopsis Ds/Spm- or T-DNA-tagged homozygous lines for nuclear-encoded chloroplast proteins, and their systematic phenotype analysis. *Plant J* 61:529–542.
30. Rüdiger W (1992) Last steps in chlorophyll biosynthesis: Esterification and insertion into membrane. *Regulation of Chloroplast Biogenesis*, ed Argyroudi-Akoyunoglou JH (Plenum Press, New York), pp 183–190.
31. Shpilyov AV, Zinchenko VV, Shestakov SV, Grimm B, Lokstein H (2005) Inactivation of the geranylgeranyl reductase (ChlP) gene in the cyanobacterium Synechocystis sp. PCC 6803. *Biochim Biophys Acta* 1706:195–203.
32. Heddad M, et al. (2006) Differential expression and localization of early light-induced proteins in Arabidopsis. *Plant Physiol* 142:75–87.
33. Peltier JB, Ytterberg AJ, Sun Q, van Wijk KJ (2004) New functions of the thylakoid membrane proteome of Arabidopsis thaliana revealed by a simple, fast, and versatile fractionation strategy. *J Biol Chem* 279:49367–49383.
34. Stagljar I, Korostensky C, Johnsson N, te Heesen S (1998) A genetic system based on split-ubiquitin for the analysis of interactions between membrane proteins in vivo. *Proc Natl Acad Sci USA* 95:5187–5192.
35. Joyard J, et al. (2009) Chloroplast proteomics and the compartmentation of plastidial isoprenoid biosynthetic pathways. *Mol Plant* 2:1154–1180.
36. Rüdiger W (1997) Chlorophyll metabolism: From outer space down to the molecular level. *Phytochemistry* 46:1151–1167.
37. Iwai M, Takahashi Y, Minagawa J (2008) Molecular remodeling of photosystem II during state transitions in Chlamydomonas reinhardtii. *Plant Cell* 20:2177–2189.
38. Koch M, et al. (2004) Crystal structure of protoporphyrinogen IX oxidase: A key enzyme in haem and chlorophyll biosynthesis. *EMBO J* 23:1720–1728.
39. Tanaka R, Tanaka A (2007) Tetrapyrrole biosynthesis in higher plants. *Annu Rev Plant Biol* 58:321–346.
40. Gehl C, Waadt R, Kudla J, Mendel R-R, Hänsch R (2009) New GATEWAY vectors for high throughput analyses of protein-protein interactions by bimolecular fluorescence complementation. *Mol Plant* 2:1051–1058.
41. Wittig I, Braun H-P, Schägger H (2006) Blue native PAGE. *Nat Protoc* 1:418–428.